

ACTIVE DAMPING IN LCL-FILTERED GRID CONVERTERS USING SOGI-BASED CAPACITOR VOLTAGE FEEDBACK

Hareesh Kumar Yada¹, Ajay Kumar Niligonda², Martha Rajender³

¹Associate Professor, ^{2,3}U.G Scholar, Department of Electrical Engineering

Vaagdevi College of Engineering

ABSTRACT

The capacitor voltage feedback active damping control is an attractive way to suppress LCL-filter resonance especially for the systems where the capacitor voltage is used for grid synchronization, since no extra sensors are added. The derivative is the core of the capacitor voltage feedback active damping control. However, in digital systems, the discrete implementation of the derivative suffers from noise amplification and accuracy issues. To overcome these drawbacks, this paper proposes a new derivative method based on Second-Order Generalized Integrator. Theoretical study shows that the proposed derivative is more suited for capacitor voltage feedback active damping control. Perturb and observe method is used as mppt algorithm for PV to grid synchronization.

Keywords: Active damping; LCL-filter; Matlab/Simulink; Photovoltaic; Second-order generalized integrator

I. INTRODUCTION

Photovoltaic (PV) modules are used to generate electricity from light. When sunlight falls on the PV modules, it converts sun light into DC electricity. Apart from the benefits of renewable energy sources, the PV based power generation has few more added benefits. The PV based system has no wear and tear which ends up in less maintenance. The PV based systems are utilized in stand- alone applications like street lighting, water pumping and additionally accommodated in grid connected systems. A circuit based system model of PV modules helps to analyze the performance of commercial PV modules. Modeling of photovoltaic modules or arrays is bestowed in numerous papers. simple circuit based PV models are planned in [1-2].The methods of adjusting I-V characteristics of the model using artificial intelligence is bestowed in [3-4]. The model of PV module based on the circuit model and its mathematical equation using basic blocks is developed in MATLAB/Simulink [5]. Matlab program based PV module is bestowed in [6]. to overcome this disadvantage, the alternative active damping (AD) technique is considered, whose basic plan is to use a virtual resistor to mimic the physical one. The AD solutions are usually realized by feeding back additional filter variables to this controller output as damping terms. The feedback variables can be capacitor current [7]–[8], capacitor voltage [9], [10], and grid current [11], [12]. which variable to choose depends on the current and voltage levels as well as the applications

[9]. The capacitor voltage feedback ought to be selected in 2 cases: 1) the current sensors are way more costly than the voltage sensors when the power level is MW range and the voltage is under 1000 V [9]. during this case, the condenser voltage feedback AD technique ought to be hand-picked. 2) The condenser voltage is used for grid synchronization once the grid-side inductor is looked as a part of the feeder impedance [13]. during this case, the capacitor voltage feedback AD is preferred, since no extra sensors are added for resonance damping. Reference [9] shows that, among proportional, derivative, and integral capacitor-voltage feedback, only the derivative feedback of the capacitor voltage can achieve resonance damping. However, the digital implementation of derivative is often a challenge [9], [14], that limits the utilization of the capacitor Voltage derivative Feedback (CVDF) AD method.

To avoid the drawbacks of the conventional digital derivatives, this paper proposes an improved digital derivative, that relies on the Second-Order Generalized integrator (SOGI). The SOGI was used widely in grid synchronization in recent years [15]. However, applying SOGI for derivative has not been reported in the literature. The planned derivative method has both high- and low-frequency noise attenuation abilities, which is more appropriate for the CVDF AD control. Moreover, the proposed derivative also helpful in alternative applications wherever signals with particular frequencies need to be differentiated. in the following, the principle of the SOGI based derivative used in CVDF AD control is explained and also the effectiveness of the proposed method is evaluated by simulink.

II. EQUIVALENT CIRCUIT OF A SOLAR CELL

The solar cell can be represented by the electrical model shown in Figure 1

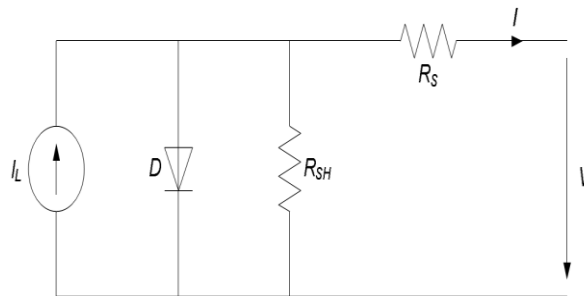


Fig.1 Equivalent circuit of solar cell.

Its mathematical equations can be expressed by the following equations:

$$I = I_L - I_0 \left(e^{\frac{q(V-IR_S)}{AKT}} - 1 \right) - \frac{V - IR_S}{R_{SH}}$$

where I and V are the solar cell output current and voltage respectively, I_0 is the dark saturation current, q is the charge of an electron, A is the diode quality (ideality) factor, k is the Boltzmann constant, T is the absolute temperature and RS and RSH are the series and shunt resistances of the solar cell.

The maximum power is generated by the solar cell at a point of the current-voltage characteristic where the product VI is maximum. This point is known as the MPP and is unique, as can be seen in Figure 2, where the previous points are represented.

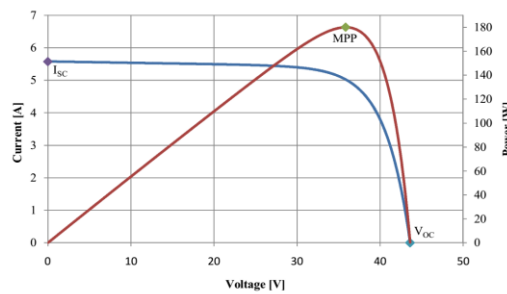


Fig.2 Important points in the characteristic curves of a solar panel

Temperature and irradiance effects

The MPP varies during the day and that is the main reason why the MPP must constantly be tracked and ensure that the maximum available power is obtained from the panel. The effect of the irradiance on the voltage-current (V-I) and voltage-power (V-P) characteristics is depicted in Figure 3, where the curves are shown in per unit, i.e. the voltage and current are normalized using the V_{OC} and the I_{SC} respectively, in order to illustrate better the effects of the irradiance on the V-I and V-P curves.

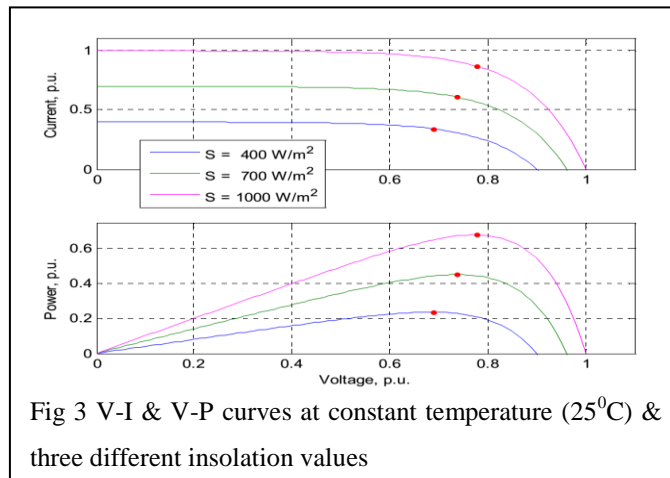


Fig 3 V-I & V-P curves at constant temperature (25⁰C) & three different insolation values

Figure 4 shows how the voltage-current and the voltage-power characteristics change with temperature. The curves are again in per unit, as in the previous case.

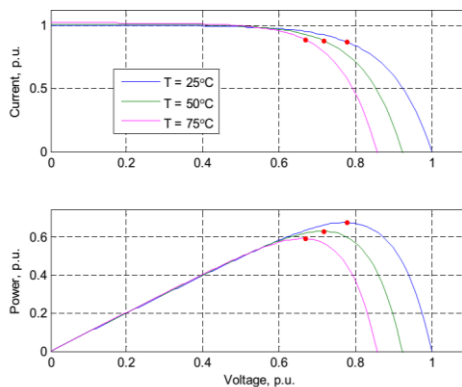


Fig 4 -V-I and V-P curves at constant irradiation (1kW/m²) and three different temperatures.

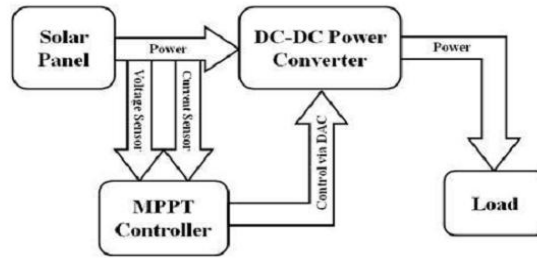


Fig: Block diagram of MPPT

One of the most successful and simplest methods for MPPT is the Perturb and Observe (P&O) method (Femia et al., 2004). In this approach, the controller works by perturbing the PV array output voltage and observing the effect on the output PV power. There are a number of variants of P&O algorithm which are reported in the literature. As can be seen in Figure, on the left of the MPP incrementing the voltage increases the power whereas on the right decrementing the voltage increases the power.

If there is an increment in the power, the perturbation should be kept in the same direction and if the power decreases, then the next perturbation should be in the opposite direction. Based on these facts, the algorithm is implemented. The process is repeated until the MPP is reached. Then the operating point oscillates around the MPP.

III.SYSTEM DESCRIPTION

Fig. 5 shows the general circuit diagram and control system of a three-phase grid-connected VSC with LCL-filter. In Fig. 1, L1 is the converter-side inductor, L2 is the grid-side inductor, Lg is the grid inductance, and Cf is the filter capacitor. The equivalent series resistances of the inductors and capacitors are neglected to draw the worst case. The grid current i2 is regulated to control the injected power into the grid. The capacitor voltage Vc is sensed for both grid synchronization and resonance damping. Alternatively, the resonance can also be damped by measuring the capacitor current instead, but would require additional three-phase current sensors.

The s-domain transfer function relating to the converter output voltage v and the grid current i2 is given by

$$G_{i2}(s) = \frac{i_2(s)}{V(s)} = \frac{1}{sL_1(L_g + L_2)C_f s^2 + w_r^2} \quad (1)$$

where w_r is the resonance frequency and can be calculated as

$$w_r = \sqrt{\frac{L_1 + (L_g + L_2)}{L_1(L_g + L_2)C_f}} \quad (2)$$

The s-domain transfer function relating to the converter output voltage v and the capacitor current v_c is given by

$$G_{v_c}(s) = \frac{V_c(s)}{V(s)} = \frac{1}{L_1 C_f s^2 + w_r^2} \quad (3)$$

The transfer function relating V_c to i₂ can be developed by calculating the ratio of (1) and (3), which is given by

$$\frac{i_2(s)}{V_c(s)} = \frac{G_{i2}(s)}{G_{v_c}(s)} = \frac{1}{s(L_g + L_2)} \quad (4)$$

Active damping can be achieved by feeding back the capacitor current. In order to avoid additional current sensors, the capacitor current can be estimated from the derivative of the capacitor voltage [10]. As for the

CVDF AD control system, when time delays are neglected, the transfer function relating to grid current i_2 and controller output voltage u can be given by

$$G_{ad}(s) = \frac{i_2}{u} = \frac{1}{sL_1(L_g + L_2)C_f s^2 + s\left(\frac{K_a}{L_1}\right) + w_{r2}} \quad (5)$$

Compared with (1), the natural resonance frequency of (5) remains but an additional damping term is obtained. Thus, resonance damping is achieved.

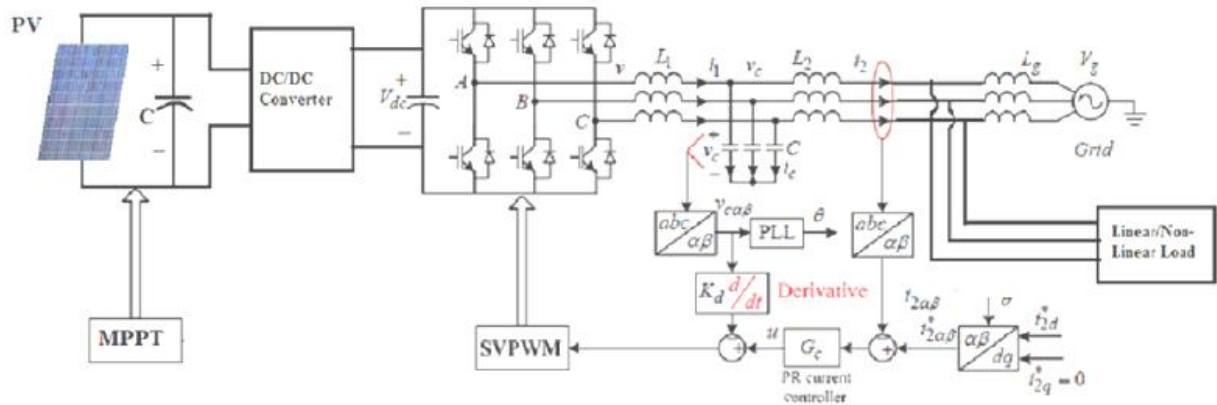


Fig.5: Schematic of LCL-filtered VSC and grid current control with an inner CVDF Active Damping (AD) loop.

IV. PROPOSED SOGI-BASED DERIVATIVE

According to the previous analysis, backward-Euler derivative suffers from large phase error, which limits its usage in CVDF AD control. The lead-lag derivative can have smaller phase error by selecting an appropriate parameter. But its discretized version narrows the effective damping region and the additional grid impedance estimation algorithm will complicate the overall control system. To overcome these drawbacks, this paper proposes a new SOGI-based derivative method.

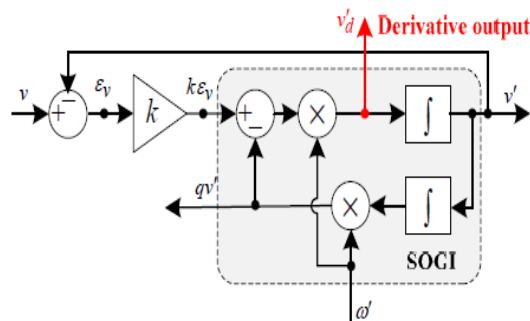


Fig.6 Basic SOGI layout.

The structure of the SOGI-based derivative method is shown in Fig. 6, where v' and qv' are the in-phase and in-quadrature signals of the input signal v , while ω' and k are the center frequency and the damping factor of SOGI. The transfer function relating v' to v is given by

$$G_v(s) = \frac{v'}{v} = \frac{Kw's}{s^2 + Kw's + w'^2} \quad (7)$$

Now that v' has the same magnitude and phase as v at the frequency \hat{A}' , it is easy to find that vd' is the derivative of the input v at the frequency \hat{A}' . When used for CVDF AD control, the 90° -crossing frequency \hat{A}' should be set at the LCL-filter resonance frequency, which is similar to lead-lag derivative. The transfer function relating vd' to v is given by (8). The Tustin transformation prewrapped at the resonance frequency is adopted to discretize (8).

$$G_{v'd}(s) = \frac{V'_d}{V} = \frac{Kw's^2}{s^2 + Kw's + w'^2} \quad (8)$$

However, as mentioned previously, the SOGI-based derivative also needs additional grid impedance estimation algorithm to calculate the resonance frequency, since it only has the derivative characteristic at a specific frequency. The grid impedance estimation algorithm will however make the overall control system complicated, so it is meaningful to investigate whether the SOGI-based derivative can work without the grid impedance estimation.

TABLE:

Sampling frequency	f_s	10 kHz
Grid inductance	L_g	0mH or 1mH
Converter -side-inductor	L_1	2mH
Filter capacitor	C_f	5uF
Grid-side inductor	L_2	1mH
Resonance frequency	f_r	2.76kHz($L_g=0mH$) 2.25kHz($L_g=1mH$)

V. SIMULATION RESULTS

The simulation results show the performance of the Photovoltaic system and boost converter with a grid connected inverter. Fig.7 shows the boost voltage, fig. 8 shows the PV Voltage and Fig. 9 shows the PV current. The load is made unbalanced and also tested under unbalanced conditions shown in Fig.10,

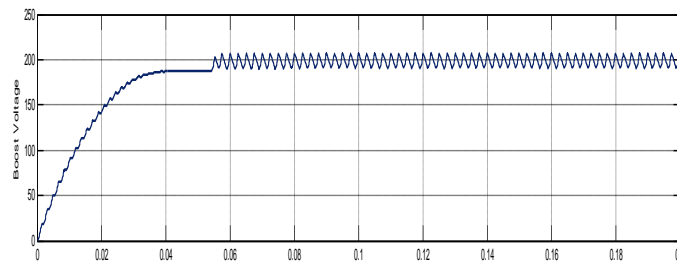


Fig 7. Boost voltage

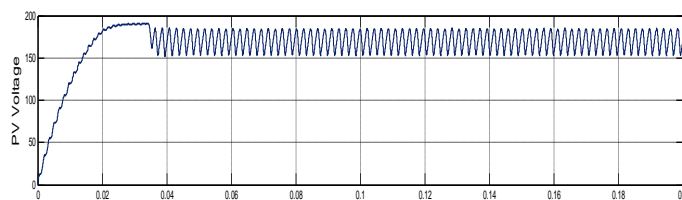


Fig. 8. PV Voltage

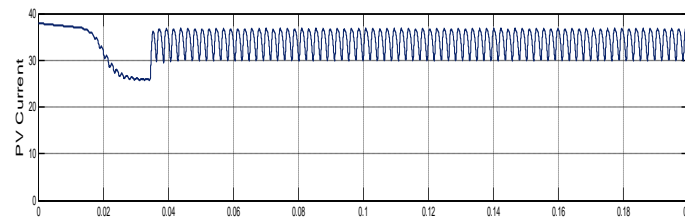


Fig. 9. PV Current

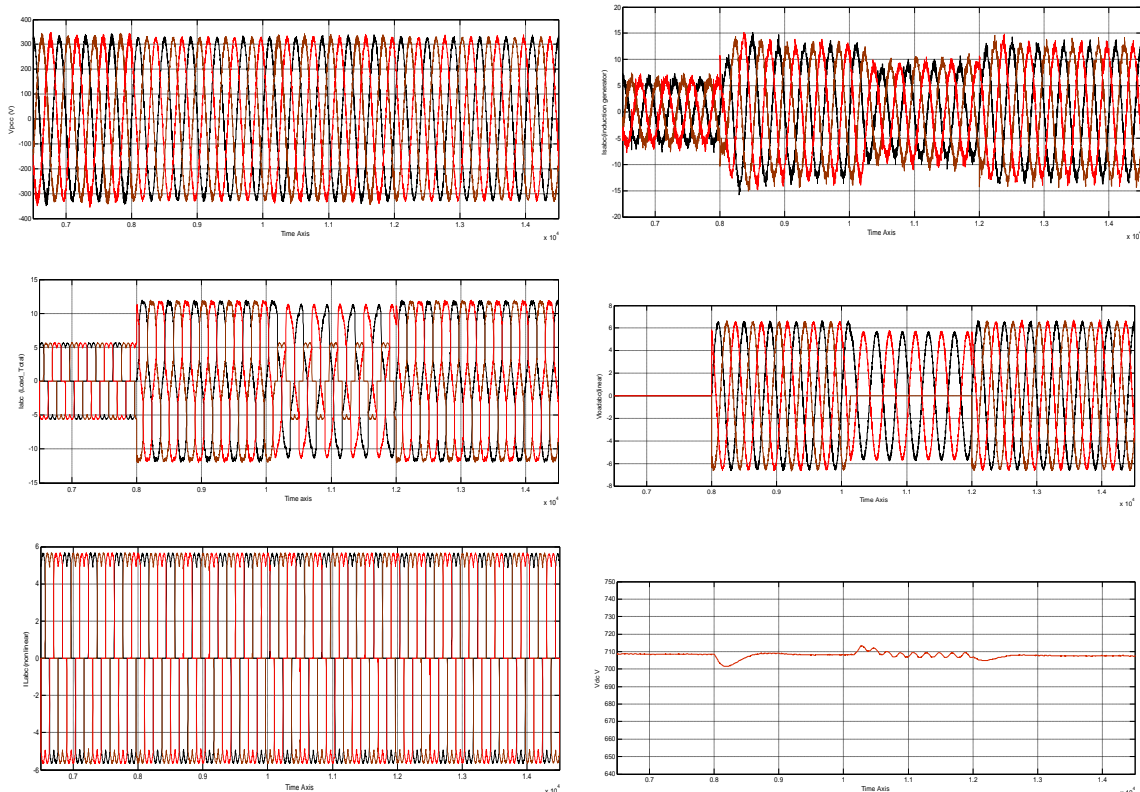


Fig.10. Simulation results for the considered system showing source voltage (V_{sabc}), source currents (i_{sabc}), load currents ($i_{load_total}=i_{load_nonlinear}+i_{load_linear}$), battery voltage and voltage across DC capacitor connected across the inverter are constant given as (V_{dc})

VI. CONCLUSION

In this paper, Grid synchronization of PV is done with filtering capabilities using an LCL filter. Active damping is also done based on the capacitor voltage feedback using a second order generalized integrator. This proposed method enhanced the stability of the system with an appropriate parameter design. The PV is supplied to a boost converter with P&O mppt algorithm for better results. The simulation results under distorted load conditions are also shown and the controller is working effectively.

REFERENCES

- [1] J.A.Gow, C.D.Manning, “ Development of photovoltaic array model for the use in power electronic simulation studies,” IEE Proceedings Electric power applications, Vol. 146, No.2, March,1999.

- [2] Jee-Hoon Jung, and S. Ahmed, "Model Construction of Single Crystalline Photovoltaic Panels for Real-time Simulation," IEEE Energy Conversion Congress & Expo, September 12-16, 2010, Atlanta, USA.
- [3] T. F. Elshatter, M. T. Elhagry, E. M. Abou-Elzahab, and A. A. T. Elkousy, "Fuzzy modeling of photovoltaic panel equivalent circuit," in Proc. Conf. Record 28th IEEE Photovoltaic Spec. Conf., pp. 1656–1659, 2000.
- [4] M. Balzani and A. Reatti, "Neural network based model of a PV array for the optimum performance of PV system," in Proc. Ph.D. Res. Microelectron. Electron., vol. 2, pp. 123–126, 2005.
- [5] S. Sheik Mohammed, "Modeling and Simulation of Photovoltaic module using MATLAB/Simulink" International Journal of Chemical and Environmental Engineering, 2011
- [6] Francisco M. González-Longatt, "Model of Photovoltaic Module in Matlab™" 2do congreso iberoamericano de estudiantes de ingeniería eléctrica, electrónica y computación (ii cibelec 2005)
- [7] D. Pan, X. Ruan, C. Bao, W. Li, and X. Wang, "Optimized controller design for LCL-type grid-connected inverter to achieve high robustness against grid-impedance variation," IEEE Trans. Ind. Electron., vol. 62, no. 3, pp. 1537–1547, Mar. 2015.
- [8] R. Pena-Alzola, M. Liserre, F. Blaabjerg, R. Sebastian, J. Dannehl, and F. W. Fuchs, "Systematic design of the lead-lag network method for active damping in LCL-filter based three phase converters," IEEE Trans. Ind. Inf., vol. 10, no. 1, pp. 43–52, Feb. 2014.
- [9] X. Wang, F. Blaabjerg, and P. C. Loh, "Analysis and design of gridcurrent-feedback active damping for LCL resonance in grid-connected voltage source converters," in Proc. of IEEE ECCE, 2014, pp. 373–380.
- [10] J. Xu, S. Xie, and T. Tang, "Active damping-based control for gridconnected LCL-filtered inverter with injected grid current feedback only," IEEE Trans. Ind. Electron., vol. 61, no. 9, pp. 4746–4758, Sep. 2014.
- [11] J. He and Y. Li, "Generalized closed-loop control (GCC) schemes with embedded virtual impedances for voltage source converters with LC or LCL filters," IEEE Trans. Power Electron., vol. 27, no. 4, pp. 1850–1861, Apr. 2012.
- [12] L. Harnefors, A. G. Yepes, A. Vidal, and J. Doval-Gandoy, "Passivitybased controller design of grid-connected VSCs for prevention of electrical resonance instability," IEEE Trans. Ind. Electron., vol. 62, no. 2, pp. 702–710, Feb. 2015.
- [13] V. Blasko and V. Kaura, "A novel control to actively damp resonance in input LC filter of a three-phase voltage source converter," IEEE Trans. Ind. Appl., vol. 33, no. 2, pp. 542–550, Mar. 1997.
- [14] P. Rodriguez, A. Luna, I. Candela, R. Teodorescu, and F. Blaabjerg, "Grid synchronization of power converters using multiple second order generalized integrators," in Proc. 34th Annu. Conf. IEEE Ind. Electron., Nov. 2008, pp. 755–760.
- [15] J. Wang, J. Yan, L. Jiang, and J. Zou, "Delay-dependent stability of single-loop controlled grid-connected inverters with LCL filters," IEEE Trans. Power Electron., [online].